MORPHOLOGY AND MECHANICAL PROPERTIES IN SEMICRYSTALLINE POLYMERS

E. H. ANDREWS

Department of Materials, Queen Mary College, London E1 4NS, UK

ABSTRACT

The application of composite theories to relationships between mechanical properties and structure in semicrystalline polymers is considered. The approach is illustrated by recent results from the author's laboratories for three classes of polymer morphology, namely spherulitic (polyethylene), row nucleated (*cis*-polyisoprene) and fibrillar (solid-state polymerized polyoxymethylene). The success of the approach emphasizes that semicrystalline polymers can nearly always be represented morphologically as consisting of separate and mechanically distinct crystalline and amorphous phases.

1. INTRODUCTION

The high level of interest in man-made composite materials has, especially during the last decade, given rise to many attempts to relate their mechanical behaviour to that of the constituent phases. To this end, many theoretical contributions have been made which can be summarized by the term 'composite theory' or 'micromechanics theory'. These theoretical developments have, in the main, concentrated on the elastic moduli of two-component systems exhibiting Hookean elasticity and are exemplified by the now-classical diagram shown in *Figure 1*. This diagram shows the Young's modulus predicted as a function of composition for a particular choice of the ratio, E_1/E_2, of the moduli of the components. The diagram shows four curves each of which corresponds to a particular 'morphological model' or set of assumptions regarding the stress or strain distribution.

The curve marked V is that first derived by Voigt[1] on the assumption that the strain is uniform throughout both phases. This corresponds to a model with the phases in parallel (e.g. infinite rods of one phase aligned in the direction of strain, embedded in a matrix of the second phase), and represents the stiffest possible structure in the absence of other constraints[2,3]. Alternatively, the Reuss model[4] which gives the curve marked R in *Figure 1* represents the behaviour of a system in which the *stress* is equal in the two components. An example of this morphology is a sandwich structure of alternating layers of the two phases loaded normal to the plane of the layers. We shall be referring later to this sandwich morphology.

The Voigt and Reuss models provide upper and lower bounds respectively, but their predictions differ so greatly for E_1/E_2 values significantly different from unity, that they are of rather academic interest. Attempts to improve

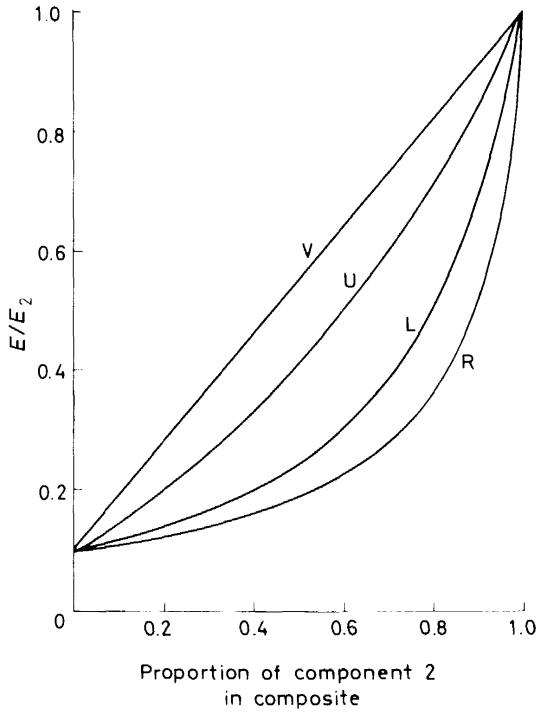

Figure 1. An example of Voigt, Reuss and Hashin-Shtrikman upper and lower bounds for the modulus of a two-component composite. Modulus expressed as E/E_2 for $E_2/E_1 = 10$.

the definition of the modulus, i.e. to define closer upper and lower bounds, have been energetically pursued, with much success. Hashin[5] and Hashin and Shtrikman[6] treated the case of spherical and non-spherical inclusions of one phase embedded in the second and used variational principles to predict upper (U) and lower (L) bounds for the elastic moduli as a function of composition. These are shown in *Figure 1* for the Young's modulus of a composite with arbitrary phase geometry, and define much narrower bounds than the Voigt and the Reuss models. Although these results, based on very general considerations, are valuable, more precise predictions require the exact specification of the morphology, i.e. the shape, distribution and concentration of the phases.

The application of these concepts to naturally occurring 'composite' materials poses a number of difficulties. Most such materials have microstructures which require sophisticated methods for their definition, either on account of the very small scale on which they occur or because mechanically important features are not readily discerned (e.g. by microscopy). Secondly, it may be impossible to isolate the separate phases to measure the *single*-phase properties. Even where comparable single-phase solids exist, it is difficult to ensure that they exhibit identical properties to those of the

in-situ composite phase. Thirdly, it may be difficult to control the phase composition and/or geometry to obtain systematic variations in properties. Examples of some of these difficulties are found in the prediction of elastic moduli for bone (a natural composite of collagen and hydroxyapatite), discussed by Katz[7], and the problem of characterizing the amorphous phase in polyethylene (see later). The inaccessibility of the separate phases to mechanical characterization, of course, provides an 'escape route' by which to explain discrepancies between theory and experiment, and such discrepancies *may* betray the presence of previously unsuspected morphological features (e.g. Krigbaum, Roe and Smith[8]). However, this remains an unsatisfactory feature of our current state of knowledge.

In the face of morphological uncertainties, it is tempting to adopt a 'curve-fitting' approach using a general model which is not intended to relate directly to the actual morphology of the system. Some success was obtained by this means by Mullins and Tobin[9] and by Takayanagi[10] who used a combined series and parallel spring model. Until, however, we are able to employ models which correspond in some way to the known morphologies, the application of composite theory to such systems as semicrystalline polymers seems of doubtful value.

Attempts to use morphologically realistic models for semicrystalline polymers have recently been made by Reed[11] for *cis*-polyisoprene and by Halpin and Kardos[12] for model spherulitic and layered polymers. Although Halpin and Kardos used only artificial composites, their work provided a starting point for the investigations of Patel and Phillips[13] reviewed below and focused attention on the possibility of treating spherulitic polymers by a simple two-phase composite theory.

In what follows, some further examples are given in which realistic morphological models have been used to predict, quantitatively where possible, the Young's moduli of semicrystalline polymers. These models vary from that of Halpin and Kardos, in which a spherulite is represented as an isotropic array of crystalline filaments in an amorphous matrix, to one in which the polymer is represented by a system of packed parallel filaments of varying aspect ratio. In each case the composite concept of distinct crystalline and amorphous phases appears valid and is sometimes highly successful.

This emphasizes the validity of distinct-phase morphologies for semicrystalline polymers, not only in low crystallinity materials where microscopy reveals graphically the separation of the phases[14], but also in high crystallinity materials (crystallinity in excess of 90 per cent). It appears that single-phase concepts such as paracrystallinity have yet to prove any advantage over 'composite' concepts in predicting the mechanical properties of even highly crystalline polymer solids.

2. YOUNG'S MODULUS OF SPHERULITIC POLYETHYLENE

2.1 Theoretical equations

The appropriate equations are those derived by Halpin and Kardos[12] for the Young's modulus, E_{11}, of an oriented array of ribbon-like crystal

lamellae, of longitudinal Young's modulus E_c, embedded in an isotropic matrix of amorphous material, modulus E_m. The equations are:

$$E_{11}/E_m = (1 + \xi\eta v_f)/(1 - \eta v_f) \tag{1}$$

and

$$\eta = \frac{(E_c/E_m) - 1}{(E_c/E_m) + \xi} \tag{2}$$

where v_f is the volume fraction of crystalline material and ξ is the aspect ratio of the lamellae (ratio of twice the length to the thickness of the ribbon). For a spherulitic polymer containing radiating lamellae it seems reasonable to equate ξ to the spherulitic diameter divided by the lamellar thickness.

It follows from equations (1) and (2) that

$$\frac{E_{11} - E_m}{E_{11} + \xi E_m} = \eta v_f \tag{3}$$

and a plot of the left hand side of equation (3) against η should give a straight line of slope v_f. In order to apply these equations to the isotropic array of filaments appropriate to a spherulitic solid, it is assumed that $E_{11} \gg E_{22}, G_{12}$ (the Young's and shear moduli in the perpendicular and parallel directions respectively). Then E_{11} can be taken as approximately three times the isotropic Young's modulus, E, of the spherulitic polymer.

Equations (1) and (2) apply over certain ranges of ξ only. Halpin and Kardos predict that E should become constant at $\xi \geqslant 1000$.

These predictions will be considered later in the light of the experimental data on high-density polyethylene. In order to apply the predictions it has been assumed that E_c is the Young's modulus in the b crystallographic direction[15]

$$E_c = 4000\ \text{MN m}^{-2}$$

and that the matrix modulus is of the order of that of a typical elastomer,

$$E_m = 10\ \text{MN m}^{-2}$$

2.2 Experimental Programme

Dumb-bell specimens were cut from compression moulded sheets of a standard high-density polyethylene supplied by the Polymer Supply and Characterisation Centre, RAPRA, Shawbury. These specimens were placed in close-fitting moulds and heated to 200 °C in a vacuum for 2 h before being quenched to the desired crystallization temperature, where they were held for 24–36 h depending on the temperature. In order to generate small spherulite sizes, repeated quenching from just above the melting point was employed to increase the nucleation density by self-seeding.

Mechanical properties were determined at 23 °C using an Instron tester and true-stress–true-strain analysis. Young's modulus was determined over the first one per cent strain and results are the average from six specimens at each condition.

Spherulite radii were determined using laser-light scattering[16], the results

occasionally being checked by polarizing microscopy. The two methods always agreed within 25 per cent. Lamellar thicknesses were calculated by using the specimen melting points (obtained by DTA) together with data[17] from the literature relating lamellar thickness to melting point. Results were confirmed for selected specimens using low-angle x-ray diffraction, which agreed within ten per cent.

Finally, further specimens were prepared and tested to explore the variation of modulus with lamellar thickness at constant spherulite radius. Materials with a spherulite radius at 9.0 μm were annealed at various temperatures to induce different degrees of lamellar thickening. Degree of crystallinity was estimated in all cases by density measurements.

2.3 Results

Figure 2 shows the variation of Young's modulus with spherulite radius for 'as crystallized' specimens, and reveals a threefold difference between the moduli of the softest and stiffest specimens. This large difference is unlikely to be a result of crystallinity variations since the measured values of v_f varied only between 67 and 77 per cent and this variation was not systematic. Secondly, a clear maximum is found at a mean spherulite radius of about 13 μm.

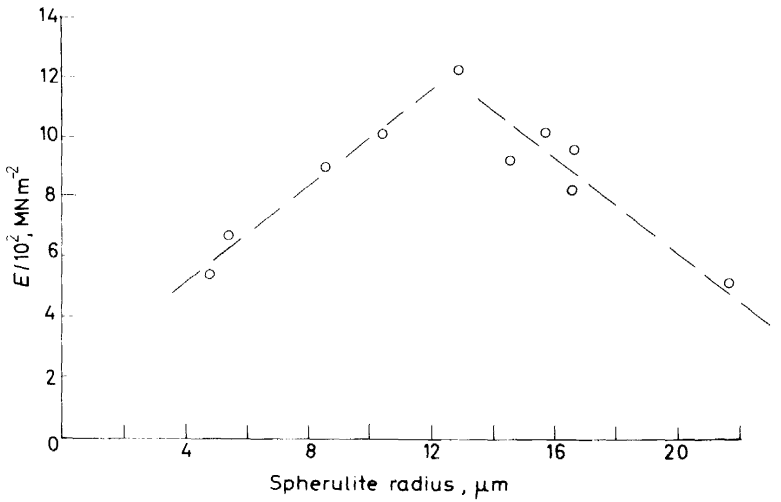

Figure 2. Young's modulus of a spherulitic polyethylene as a function of spherulitic radius (after Patel and Phillips).

This interesting result is consistent with the picture suggested by Halpin and Kardos[12], since the initial increase in modulus with spherulite size occurs in specimens crystallized at supercoolings in excess of 20°C, in which range the lamellar thickness is insensitive to temperature. Thus these lamellae have aspect ratios which are nearly proportional to the spherulite radius, and the near-proportionality of Young's modulus and spherulite size (*Figure 2*) is a direct result. At higher temperatures (supercoolings less

than 20°C), even larger spherulites are obtained but now the lamellar thickness is increasing rapidly with crystallization temperature. The tendency to higher aspect ratios arising from larger spherulite radii is thus offset and eventually swamped by the decrease in ξ caused by rising lamellar thickness, so that ξ and modulus begin to decrease with increasing spherulite size. The maximum in *Figure 2* results.

This explanation is strongly supported by the data given in *Figure 3*

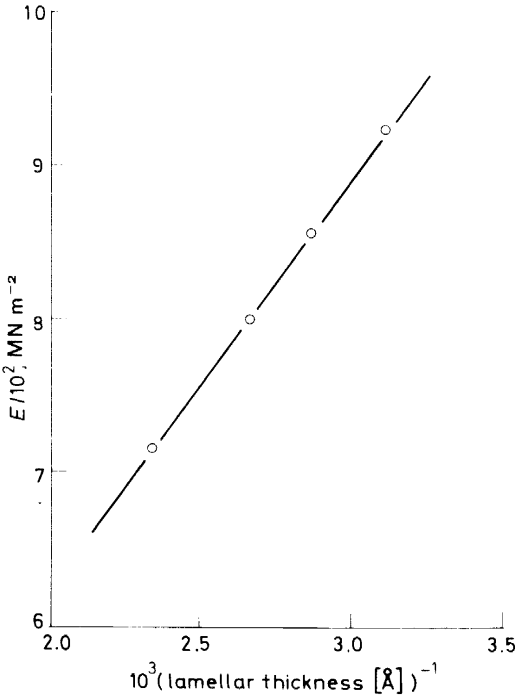

Figure 3. Young's modulus of a spherulitic polyethylene as a function of lamellar thickness at a constant spherulitic size of 9.0 μm (after Patel and Phillips).

which reports the effect on Young's modulus of lamellar thickness at constant spherulite radius (data from annealed specimens). This shows that Young's modulus is very nearly inversely proportional to lamellar thickness in this range of ξ. Decreasing lamellar thickness thus increases ξ and increases the Young's modulus at constant spherulite radius.

The most critical test of the theory is shown in *Figures 4* and *5*. In *Figure 4* is shown the Young's modulus as a function of the aspect ratio ξ. Between $\xi = 400$ and 800, E increases sigmoidally from the lower limit for $\xi = 1$ to the theoretical upper limit for $\xi > 1000$. Although the upper limit is reached earlier than $\xi = 1000$, as given by Halpin and Kardos, and although two of the repeatedly quenched specimens lie off the line, *Figure 4* represents excellent agreement with theory.

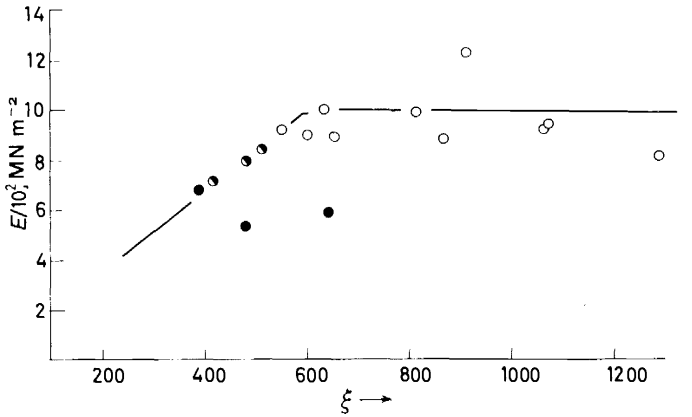

Figure 4. Young's modulus of a spherulitic polyethylene as a function of lamella aspect ratio (after Patel and Phillips); (●), repeated quench; (◔) annealed specimens.

Figure 5 shows the data plotted according to equation (3), using $E_{11} = 3E$. The slowly crystallized specimens exhibit the predicted linear dependence with a slope, v_f, falling very close to the values (0.67 to 0.77) obtained from density measurements.

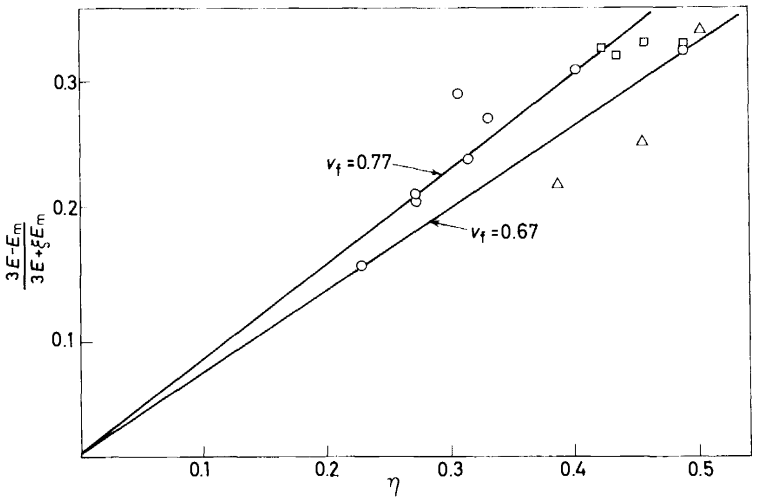

Figure 5. Data plotted according to equation (3) (after Patel and Phillips). (○) slow crystallization; (△) repeated quench; (▽) annealed specimens.

2.4 Conclusion

The main conclusion from this work is that the elastic moduli of a highly crystalline, spherulitic polymer can be explained in terms of a simple two-phase composite of crystalline filaments in an amorphous matrix. Good quantitative agreement between theory and experiment can be obtained

without invoking more sophisticated concepts such as tie-molecules or unusual amorphous states.

This is not, of course, to say that interlamellar contacts, tie molecules and the like are either unimportant or absent. Indeed, in a previous paper[18] the author has provided good evidence that the *yield* strengths of spherulitic polyethylenes are governed by the degree of interlamellar contact. The present work simply indicates that the *initial moduli* of spherulitic material owe nothing to such aspects of the microstructure.

3. STRESS–STRAIN CURVE OF ROW-NUCLEATED POLYISOPRENE

3.1 Structure of row-nucleated *cis*-polyisoprene

This has been fully documented elsewhere[19] and needs only brief mention here. If *cis*-polyisoprene (or any other crosslinked or high-viscosity polymer) is deformed in the melt and allowed to crystallize before the stress fully relaxes, an ordered structure results in which the majority of the crystalline phase consists of lamellae lying *normal* to the direction of orientation. (This, of course, means that the molecular axis in the lamellae lies *in* the orientation direction as would be expected). Providing the melt strain is not too large, only a very small amount of crystalline material is found in the row-nuclei which lie *along* the strain axis and from which the much more extensive lamellae grow outwards. It is thus possible to represent the morphology of such a material as a sandwich structure consisting of parallel layers of crystalline and amorphous material, the layers being perpendicular to the original axis of melt strain (*Figure 6*).

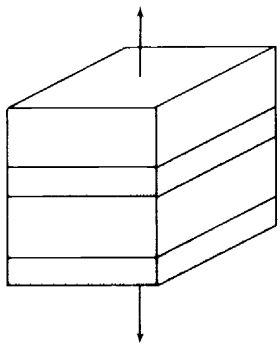

Figure 6. Sandwich model for row-nucleated *cis*-polyisoprene.

3.2 Stress–strain behaviour

Reed[11] performed tensiles tests on *cis*-polyisoprene specimens crystallized from the strained, cross-linked melt, deforming the specimens in the direction of the initial melt strain. Some results are shown in *Figure 7* (experimental points; the lines are all theoretical curves except for that marked 'amorphous'). As the diagram shows, specimens crystallized at different melt

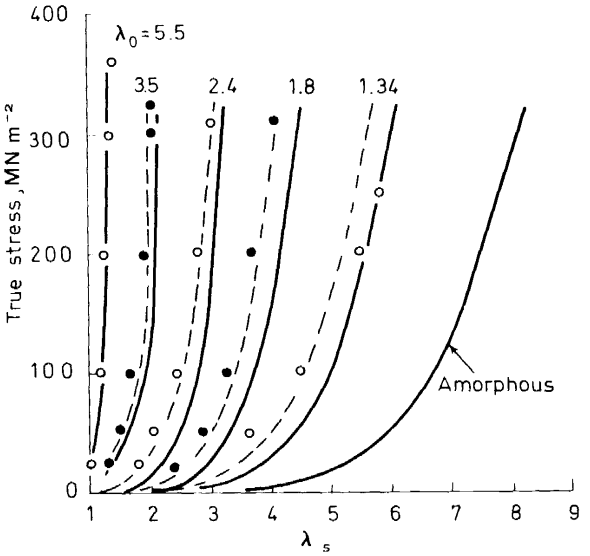

Figure 7. Stress–strain data for *cis*-polyisoprene crystallized at various melt-strains and tested at −40°C. Points and 'amorphous' curve are experimental. Other curves are theory (solid lines without lamellar buckling; broken lines with buckling) (after Reed).

strains give completely different stress–strain curves, though all are generally rubber-like reflecting the rubbery character of the amorphous phase at the temperature of test (−40°C in *Figure 7*).

At first sight the results appear incapable of explanation in terms of the sandwich model of *Figure 6*. Since the degree of crystallinity (about 30%) is nearly the same for all specimens, one would expect a single unique curve for all the crystalline specimens which would, of course, be stiffer than wholly amorphous specimens (right hand curve in *Figure 7*). Instead it is found that stiffness increases progressively as the pre-strain increases, even though the morphology and crystallinity are virtually constant. Nevertheless, as shown below, the simple composite model *can* explain all the observations, provided that the residual orientation of the amorphous phase is taken into consideration.

3.3 Theoretical explanation of the behaviour

Let the initial melt deformation be denoted by an extension ratio λ_0 (deformed length divided by undeformed length). The specimen is maintained at this extension ratio during crystallization, so that any improved molecular alignment within the growing lamellae (diffraction studies indicate almost perfect alignment in the strain direction) must be compensated by a *decrease* in molecular alignment in the amorphous layers of the sandwich. If we represent the alignments in the crystalline and amorphous regions by effective extension ratios λ_c and λ_a respectively, we have

$$\lambda_0 = v_f \lambda_c + (1 - v_f)\,\lambda_a \qquad (4)$$

where v_f is the volume fraction of crystalline phase (taken as 0.3 in this work).

λ_a here is the residual extension ratio in the amorphous zones *before* tensile testing commences. If we now suppose that deformation *during* the tensile test is restricted to the amorphous (rubber-like) phase, we have λ_s, the extension ratio of the specimen during the test, related to λ the actual extension ratio in the amorphous phase, by the following expression:

$$\lambda = \lambda_a \left\{ \frac{(1 - v_f) + \lambda_s - 1)}{(1 - v_f)} \right\} = \left(\frac{\lambda_0 - v_f \lambda_c}{1 - v_f} \right) \left(\frac{\lambda_s - v_f}{1 - v_f} \right) \tag{5}$$

which reduces, $v_f = 0.3$ being used, to

$$\lambda = 2(\lambda_0 - 0.3\lambda_c)(\lambda_s - 0.3) \tag{6}$$

If it be assumed that the amorphous phase deforms in simple extension with exactly the same stress–strain curve as the 100 per cent amorphous material (right hand curve in *Figure 7*), this equation enables us to plot λ_s against stress for the semicrystalline specimens, given a value for λ_c. This latter parameter can be calculated by using statistical theory together with the known lamellar thickness of the crystalline layers, and Reed[11] found a value $\lambda_c = 6.3$.

Reed's calculated stress–strain curves for the different pre-extensions λ_0 are shown as full lines in *Figure 7*. They provide a good qualitative representation of the data, especially with respect to the effect of λ_0 on the curve. A much better quantitative fit was obtained (dotted curves) by abandoning the unrealistic assumption that the amorphous layers deform in simple extension, without disturbing the crystalline layers. If, as must happen in practice, the crystalline layers become buckled or corrugated as a result of deformation, additional (shear) stresses are generated in the amorphous layers and allowing for these effects, calculation predicts the greater stiffness (dotted curves) actually observed experimentally. The relatively poor fit for $\lambda_0 = 1.34$ is not unexpected since at this low pre-extension the layer morphology is not yet fully developed.

3.4 Conclusion

By introducing sophistications into a very simple 'sandwich' model, the stress–strain behaviour of row-nucleated *cis*-polyisoprenes can be very satisfactorily explained. Both the model and its refinements are fully justified in terms of the known morphology and behaviour of the material, and it is suggested that herein lies the success of the approach. Once again the 'composite principles' of assuming the presence of discreet, mechanically distinct crystalline and amorphous phases provides a completely satisfactory account of the phenomena.

4. THE ELASTIC MODULUS OF SOLID-STATE POLYMERIZED POLYOXYMETHYLENE

4.1 Preparation and characterization of the polymer

Full details of this work are reported elsewhere[20, 21]. Briefly, the polyoxymethylene specimens were prepared as thick filaments (with the molecular axis aligned with the filament axis) by the solid-state polymerization of long

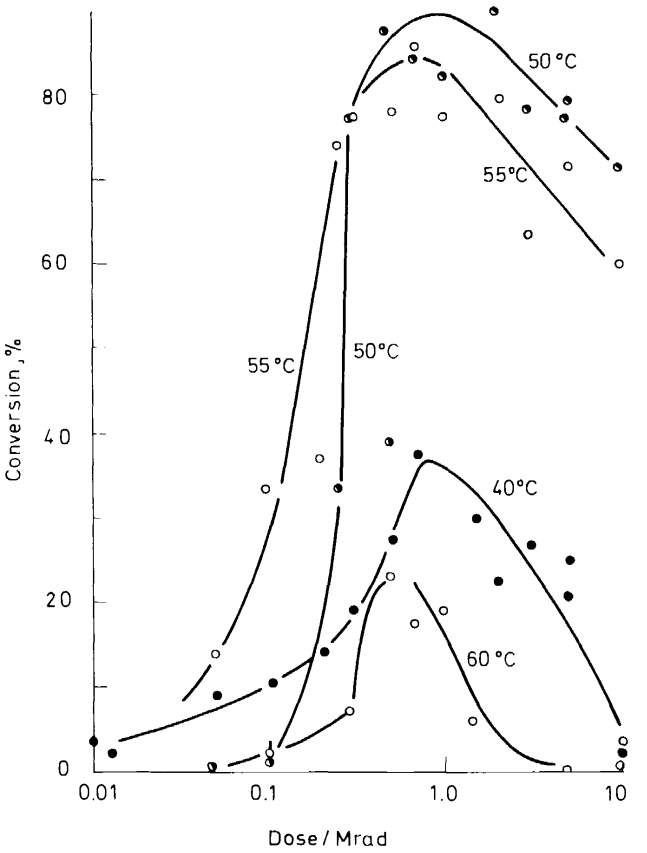

Figure 8. Degree of conversion into polymer of trioxan polymerized in the solid state at various temperatures, as a function of irradiation dose.

filamentous crystals of trioxan. The crystals were irradiated with high energy electrons at −76 °C and subsequently polymerized at fixed temperatures of 30, 40, 50, 55 and 60 °C for 48 h. *Figure 8* shows the degree of conversion into the polymeric state as a function of irradiation dose and polymerization temperature, revealing a clearly defined maximum conversion at 1 Mrad and 50–55 °C.

It is well known that, after sublimation of residual monomer, such specimens of polyoxymethylene are composed of long but discontinuous fibrils of polymer aligned in the specimen axis. The question arises as to how, and how far, such an assembly of fibrils can approach in rigidity the full theoretical stiffness of a continuous extended-chain molecular crystal.

To answer this last question, careful mechanical tensile tests were carried out on the filaments of polymer, a specially designed extensometer being used to avoid errors arising from deformation at the specimen grips (the filaments were fixed in end-blocks with an epoxy resin which has considerably greater

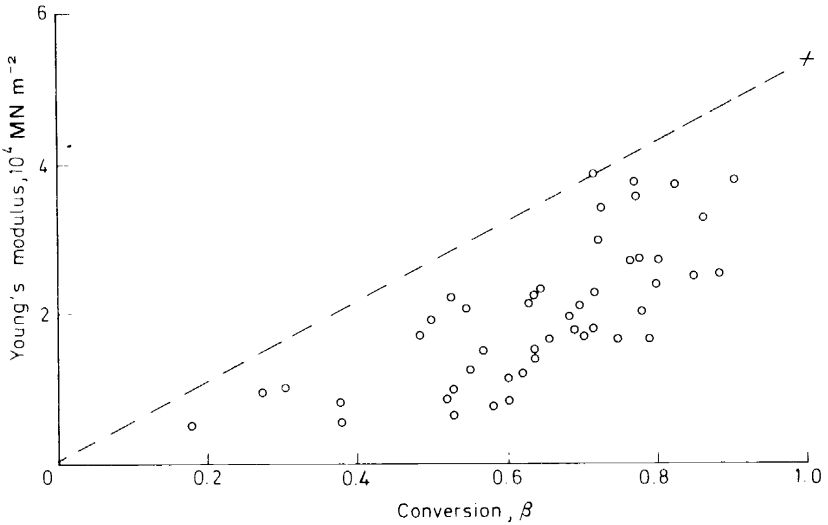

Figure 9. Young's modulus of polyoxymethylene fibres as a function of conversion. Line gives ideal behaviour for infinite micro-fibrils, extrapolating to theoretical modulus at $\beta = 1$.

compliance than the specimens themselves). Details have been given elsewhere[22].

The results for Young's modulus along the filament axis as a function of conversion, β, are given in *Figure 9*. The dotted line shows the theoretical

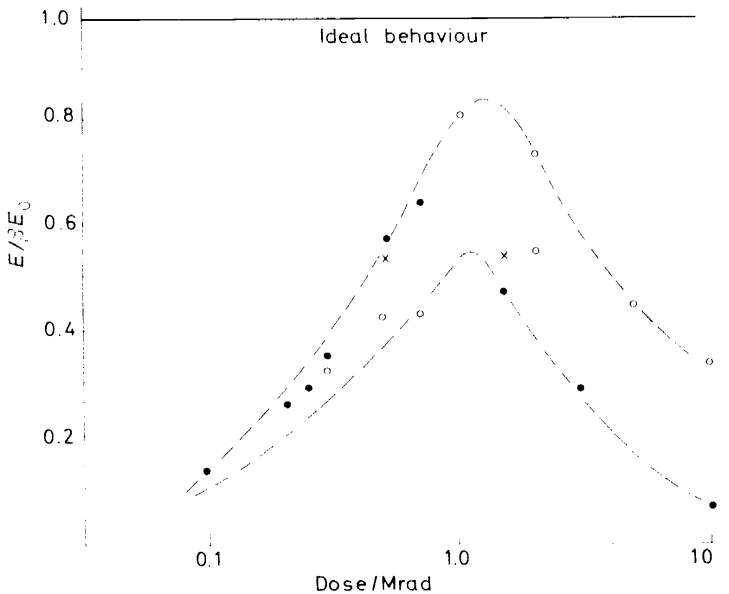

Figure 10. $E/\beta E_0$ for polyoxymethylene fibres as a function of irradiation dose; ( ) polymerized at 50; (●) at 55; (×) at 60°C.

relationship for fibrillar bundles with infinitely long fibrils, extrapolating to the theoretical modulus of the extended-chain (helical) molecular crystal of polyoxymethylene, at $\beta = 1$.

Although the fibrils which compose the filamentous specimen are known to be discontinuous, the measured moduli approach the theoretical line surprisingly closely. To further emphasize this, *Figure 10* shows a plot of Young's modulus E divided by conversion β as a function of irradiation dose (the broken lines are the envelope of experimental points). On this plot, 'theoretical modulus' for the filaments is a horizontal line and the specimens are seen to approach their theoretical stiffness under conditions where conversion is maximized. However, attempts to correlate E/β with conversion β directly are *not* successful.

Below is proposed a 'composite' model which accounts for these effects in a semi-quantitative manner and which, once again, has the virtue of being physically realistic.

4.2 Adhering fibril model for solid-state polymerized polyoxymethylene

Consider the volume of the original trioxan crystal lattice to be divided into cubic segments of cube-edge d, and suppose that conversion into polymer results in a volume fraction β of the material being converted into polymer in the form of fibrils of width d, breadth d, and length nd. The fibrils grow with a common orientation (*Figure 11*).

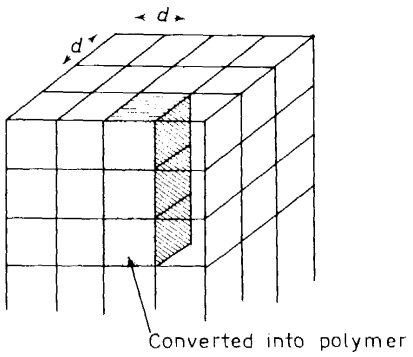

Figure 11. 'd'-Lattice for probability calculation.

Consider an element of the 'd-lattice'. The probability that it is occupied by polymer is, of course, β, and the probability that an immediately adjacent cell (in a plane perpendicular to the fibril length) is also occupied by polymer is β^2. The total side surface area of fibril is,

$$A = 4nd^2 \tag{7}$$

so that the total area of side-contact is given by

$$\beta^2 A = 4nd^2\beta^2 \tag{8}$$

The longitudinal tensile stress, σ_f, in a fibril is transferred to other fibrils only through these side contacts, the interfacial material being in shear. If G_i is the shear modulus of the interface, and the total load, $\sigma_f d^2$, on a given fibril is carried evenly by the contact regions, the interfacial strain becomes,

$$\gamma_i = \frac{\sigma_f d^2}{4nd^2\beta^2} \cdot \frac{1}{G_i} = \frac{\sigma_f}{4n\beta^2 G_i} \tag{9}$$

The total contribution, ε_i, of this shear strain to the tensile strain of the specimen is not easy to assess, since it depends upon the exact morphology of the specimen and the thickness, h, of the interface. The morphological factor can best be illustrated by *Figure 12*. In *Figure 12a* is shown a closely

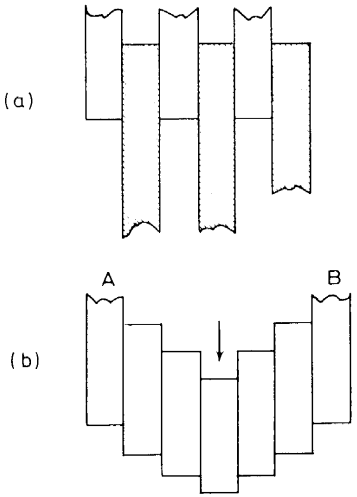

Figure 12. (a) Interleaving fibrils; (b) 'accordian' model.

packed array of fibrils which interleave, and the contribution of inter-fibrillar shear to tensile strain is of the order of

$$\varepsilon_i = \gamma_i h/nd \tag{10}$$

nd being the length of a fibril. By contrast the more open 'accordian' type structure of *Figure 12b* can contribute a maximum strain

$$\varepsilon_i = \gamma_i hN/2nd \tag{11}$$

where N is the number of fibrils between 'fixed points' A and B.

Fortunately all possibilities can be approximated by realising that N will have an average value given by,

$$N = (1 - \beta)/\beta \tag{12}$$

so that

$$\varepsilon_i = (1 - \beta)\gamma_i h/2n\beta d \tag{13}$$

The strain in the fibril itself is, of course,

$$\varepsilon_f = \sigma_f / E_0 \tag{14}$$

where E_0 is the Young's modulus of the fibril, and the total strain will therefore be

$$\varepsilon = \varepsilon_i + \varepsilon_f = \sigma_f \left\{ \frac{1}{E_0} + \frac{h(1-\beta)}{4n^2\beta^3 G_i d} \right\} \tag{15}$$

The specimen modulus is then

$$E = \frac{\beta\sigma_f}{\varepsilon} = \beta \left\{ \frac{1}{E_0} + \frac{h(1-\beta)}{4n^2\beta^3 G_i d} \right\}^{-1} \tag{16}$$

or

$$\frac{E}{\beta E_0} = \beta \left\{ \beta + \frac{E_0}{G_i} \frac{h}{d} \frac{(1-\beta)}{4n^2\beta^2} \right\}^{-1} \tag{17}$$

Unfortunately it is not possible to evaluate the right hand side of this equation with any great confidence, since G_i and (h/d) are not known. However, if plausible values are taken, E_0/G_i may be of the order of 10^3 and (h/d) of the order of 0.1, giving

$$\frac{E}{\beta E_0} \approx \left\{ 1 + \frac{100(1-\beta)}{(2n)^2\beta^3} \right\}^{-1} \tag{18}$$

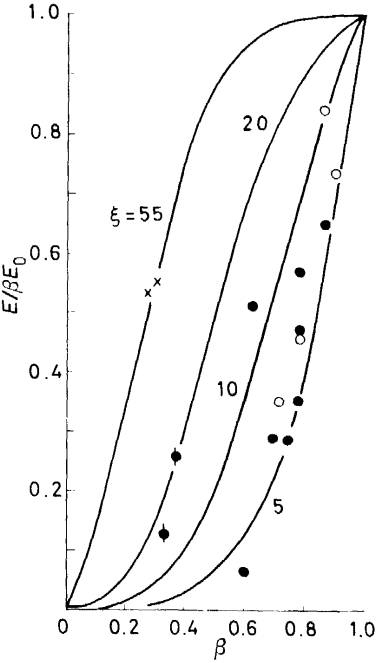

Figure 13. Fraction of theoretical modulus achieved as a function of conversion β. Points are experimental data, (○) polymerized at 50; (●) at 55; (●) at 55 low doses; (×) at 60 °C. Lines are theory for various aspect ratios $\xi = 2n$ as indicated.

the left hand side of this equation being the fraction of theoretical modulus attained for any given degree of conversion β.

The right hand side of equation (18) is plotted against β in *Figure 13* for various choices of the fibril aspect ratio ($2n$), together with experimental points. The experimental data for 50 and 55°C fit extremely well the theoretical curve for an aspect ration of 6, although the low-dose specimens polymerized at 55°C are better described by an aspect ratio of 20. The limited data for 60°C agree well with an aspect ratio of 55. It must be emphasized that the aspect ratio values for best fit are governed by the choices of E_0/G_i and of h both of which can only be guessed. The facts remain that the *form* of dependence upon β of the modulus is very well predicted by the theory, and that the aspect ratio values required to fit the data are not widely unrealistic. There is the further implication that the aspect ratio of the polymer fibrils is dependent upon the conditions of irradiation and polymerization.

4.3 Conclusion

A composite model of fibrils-in-contact is qualitatively, and to some extent quantitatively, successful in describing the deviations from theoretical values of the Young's modulus of solid-state polymerized polyoxymethylene. As in the previous cases of very different morphologies, the basic ideas of two-phase composite theory appear equal to the task of describing the deformation of semi-crystalline polymers in the elastic region. It is the author's hope that these ideas will be energetically pursued in their application to other systems.

REFERENCES

[1] W. Voigt, *Lehrbuch der Kristallphysik*, Teubner: Berlin (1910).
[2] R. Hill, *Proc. Phys. Soc. Lond.*, **A65**, 349 (1952).
[3] R. Hill, *J. Mech. Phys. Solids*, **11**, 357 (1963).
[4] A. Reuss, *A. Angew. Math. Mech.*, **9**, 49 (1929).
[5] Z. Hashin, *J. Appl. Mech.*, **84**, 143 (1962).
[6] Z. Hashin and S. Shtrikman, *J. Mech. Phys. Solids*, **11**, 127 (1963).
[7] J. L. Katz, *J. Biomechanics*, **4**, 455 (1971).
[8] W. R. Krigbaum, R. T. Roe and K. J. Smith, *J. Polymer Sci.*, **A1**, 1945 (1963).
[9] L. Mullins and N. Tobin, Proc. 3rd Rubber Technol. Conf. (London) p. 397 (1954).
[10] M. Takayanagi, *in* 4th Internat. Cong. Rheology I; ed. E. H. Lee and A. L. Copley, Wiley: New York (1965).
[11] P. E. Reed, *Ph.D. Thesis* (The influence of crystalline texture on the tensile properties of natural Rubber), University of London (1970).
[12] J. C. Halpin and J. L. Kardos, *J. Appl. Phys.*, **43**, 2235 (1972).
[13] J. Patel and P. J. Phillips, *Polymer Letters* **11**, 771 (1973).
[14] E. H. Andrews, *Proc. Roy. Soc. Lond. A*, **270**, 232 1(962).
[15] A. Odajima and A. Maeda, *J. Polymer Sci., C*, **15**, 55 (1966).
[16] M. Rhodes and R. S. Stein, *J. Appl. Phys.*, **31**, 1873 (1962).
[17] S. Kavesh and J. M. Schultz, *J. Polymer Sci. A*-2, **9**, 85 (1971).
[18] E. H. Andrews, *Pure Appl. Chem.*, **31**, 91 (1972).
[19] E. H. Andrews, *Proc. Roy. Soc. Lond., A*, **227**, 562 (1964).
[20] E. H. Andrews and G. E. Martin, *J. Material Sci.*, **8**, 1315 (1973).
[21] E. H. Andrews and G. E. Martin, *J. Material Sci.*, (submitted).
[22] G. E. Martin, *Ph.D. Thesis* (Structure and properties of polyoxymethylene polymerized in the solid state), University of London (1973).